Available online at www.ap.iauardabil.ac.ir
**Islamic Azad University, Ardabil Branch**
Anthropogenic Pollution Journal, Vol 5 (2), 2021: 93-103
10.22034/AP.2021.1936068.1114
ISSN: 2783-1736- E-ISSN: 2588-4646

ORIGINAL RESEARCH PAPER

# Organic compound removal from textile wastewater by photocatalytic and sonocatalytic processes in the presence of copper oxide nanoparticles

**Reza Fekri[1], Seyed Ahmad Mirbagheri[2], Ebrahim Fataei[3], Gholamreza Ebrahimzadeh Rajaei[4,*], Lobat Taghavi[1]**

1. Department of Environmental Science and Engineering, Faculty of Natural Resources and Environment, Science and Research Branch, Islamic Azad University, Tehran, Iran.
2. Department of Environmental Engineering, Faculty of Civil Engineering, K.N. Toosi University of Technology, Tehran, Iran.
3. Department of Environmental Science and Engineering, Ardabil Branch, Islamic Azad University, Ardabil, Iran.
4. Department of Chemistry, Ardabil Branch, Islamic Azad University, Ardabil, Iran.
***Corresponding author: Gholamreza Ebrahimzadeh Rajaei**

**Received**: 20 March 2021/ **Accepted**: 28 August 2021/ **Published**: 15 September 2021

**Abstract**
The textile industry is one of the main consumers of water and the wastewater from this industry is one of the main sources of environmental contamination because they can release high levels of organic compounds into the environment. The chemical compounds of the wastewater, especially polycyclic aromatic hydrocarbons are highly carcinogenic and toxic and must be treated before release to the environment. Photocatalytic and sonocatalytic processes in the presence of metal oxide nanoparticles (NPs) are among the advanced oxidation processes (AOPs) which have found increasing popularity due to their high efficiency and no secondary contamination. In this research, CuO NPs were first synthesized using *Peganum harmala* seed extract. The samples were then evaluated by SEM, XRD, and EDX tests. The degradation efficiency of organic compounds in textile wastewater was explored by photocatalytic and sonocatalytic processes in the presence of copper oxide NPs. The results indicated that the crystallites of the spherical CuO NPs have an average size of 84 nm. According to GC-MS results, decane, undecane, dodecane, naphthalene, decahydro-2,3-dimethyl, methylmethylenecyclohexane, decahydro-1,5-dimethyl, tridecane, tetradecane, and hexadecane composed about 73% of the initial wastewater sample. 100% of 2-methylmethylenecyclohexane, naphthalene, decahydro-1,5-dimethyl, hexadecane, and decahydro-2,3-dimethyl were eliminated by photocatalytic process. The highest (84%) and lowest (52%) sonocatalytic degradation were reported for naphthalene and/or decahydro-2,3-dimethyl, and dodecane, respectively. These values reached about 100% in photocatalytic degradation. UV waves were generally more efficient at removing organic compounds than US treatment.

**Keywords**: Organic contaminant, Copper oxide nanoparticles, Ultrasonic, Photocatalysts, Textile industry



## 1. Introduction

Water contamination, treatment of contaminated waters, and providing healthy drinkable water are the most important concerns of environmentalists, because their inadequate management has affected human societies (Shahmoradi et al., 2013). The rise in industrial and human activities has led to the discharge of huge amounts of wastewater into water resources (Ahmed et al. 2021). Among the various industries, the textile industry is one of the most polluting industries as it produces wastewaters rich in various toxic chemicals resistant to biological decomposition (Rezaee Mofrad et al., 2013). Discharge of these wastewaters into the environment without proper treatment could impose serious hazards to the environment (Yusuff et al., 2020; Arjaghi et al., 2021).

Various methods such as coagulation, ultrafiltration, reverse osmosis, ionic exchange, and adsorption on active carbon have been used to treat these wastewaters. Due to the high stability of the organic compounds and to achieve higher standards, advanced oxidation processes (AOPs) have drawn attentions (Asgari et al., 2017). Photocatalytic and sonocatalytic processes in the presence of semiconductors are among the AOPs which can efficiently convert the

organic pollutants of the aqueous media into inorganic compounds (Salavati et al., 2012).

As one of the methods of AOPs, photocatalysis decomposes the dissolved organic compounds under UV irradiation and the presence of metallic oxides (Asgari et al., 2017, Yusuff et al., 2020). This technique has found increasing popularity due to its excellent features such as nontoxicity, saving energy, ability to eliminate the contaminants from various media, degradation of diverse types of organic pollutants, and minimum production of secondary pollutants (Akerdi and Bahrami, 2019; Rezaei-Aghdam et al., 2021). Photocatalytic degradation could decompose toxic organic pollutants and convert them into completely inorganic compounds (Hasanpour and Hatami, 2020). As a result of electron excitation by high-energy photons (higher than the bandgap) in a semiconductor, electron-hole pair will be formed followed by oxidative degradation of the organic compounds. Hydroxyl radicals are the main oxidizing factor and convert these compounds into $CO_2$ and $H_2O$ and other simple inorganic ions (Al-Zahrani et al., 2020; Salavati et al., 2012).

Sonocatalysis is one of the most promising AOPs which combines ultrasonic (US) treatment with catalysis (El Hakim et al., 2021). A combination of the removal method with catalyst activities plays a decisive role in the degradation mechanism and efficiency (Fatimah et al., 2020). In this method, US waves generate hot spots inside the solution which will promote the generation of free radicals and degradation of organic pollutants (Daneshvar et al., 2019).

Semiconductors such as copper oxide have attracted a considerable deal of attention due to their physical and chemical properties. These metal oxide nanoparticles have a monoclinic structure with a band gap energy of 1.2 eV. CuO NPs have been widely employed in gas sensors, batteries, solar cells, semiconductors, and catalysts (Manasa et al., 2021). Various methods have been developed for the synthesis of NPs among which sol-gel chemical precipitation, hydrothermal, solvothermal, and microwave routes can be mentioned (Luque et al., 2020). Recently, green methods have been developed for the synthesis of metal oxide NPs using herbal extracts (Lam et al., 2021). Plants include phytochemical compounds such as phenols, flavonoids, aldehydes, and ketones whose reductive ability can convert metallic salts into metal oxide nanoparticles (Shashanka et al., 2021). Compared to other methods of synthesis, green synthesis (biosynthesis) is distinguished due to its advantages such as cost-effectiveness, accessibility, and independence from toxic reagents (Jamdagni et al., 2018; Ebrahimzadeh et al., 2012).

In this study, CuO NPs were first synthesized using *Peganum harmala* seeds extract. The synthesized NPs were then characterized by scanning electron microscopy (SEM), x-ray powder diffraction (XRD), and energy-dispersive x-ray (EDX) spectroscopy analyses to confirm the formation of CuO NPs. Sampling was conducted at the peak operation hours from the effluent of Sabalan Textile factory in Ardabil province. Using a gas chromatography–mass spectrometer (GC-MS), the compounds present in the effluent were identified. Finally, the efficiency of photocatalysis and sonocatalysis processes in the presence of CuO nanoparticles to remove existing organic compounds was investigated.

## Materials and methods

### 1.1. *Peganum harmala* extraction and synthesis of CuO NPs

*Peganum harmala* was collected from the Moghan region in Ardabil province. Then, 10 g dried seeds were mixed with 100 ml double distilled water and stirred for 30 min at 80 ℃ (RH Digital KT/C, IKA Co., Germany, 100 rpm) until reaching a brownish extract. The cooled extract was filtered (Whatman No.40, England) and stored at 4 ℃.

For the synthesis of CuO NPs, 1.7 g copper chloride dihydrate ($CuCl_2.2H_2O$, Riedel-de Haën Co., Germany) was dissolved in 100 mL distilled water and stirred for 5 min. The blue solution was mixed with 10 mL *Peganum harmala* extract and stirred for 6 h at 70 ℃ until its color changed from pale blue to dark green. To separate the solid component from the liquid phase, the sample was centrifuged (EBA 20, Hettich Co., Germany) for 30 min at 5000 rpm. The precipitants were dried at 80 ℃ in an oven (UFE 500, Memmert Co, Germany) for 12 h followed by calcination (F47, Shimi Fan Co., Iran) at 400 ℃ for 2 h until reaching black copper oxide nanoparticles (Fig. 1).


Fig. 1: Schematic overview of the synthesis of CuO NPs using *Peganum harmala* extract

### 1.2. Characterization of synthesized CuO NPs

The surface morphology of the samples was explored by scanning electron microscopy (MIRA3, TESCAN Co., Czech Republic). X-ray diffraction (XRD) analysis (PW1730, Philips Co., Netherlands) was utilized to study the crystalline structure of the samples and determine the mean particle size. The elemental composition of the NPs was examined by energy-dispersive X-ray analysis (EDX or EDS) (MIRA II, TESCAN Co., Czech Republic).

### 1.3. Effluent sampling and identification of its composition

To obtain samples, the effluent samples were collected at the peak operation hours from the main outlet of the wastewater treatment plant of the Textile factory in Ardabil province. The samples were kept at 4 ℃. The organic compounds of the samples were explored by CG-MS tests (7890A, Agilent Co., USA) operating with He at the flow rate of 1 ml/min. The type of the applied column was HP-5MS (30 m with an internal diameter of 0.25 mm) and constant phase thickness of 0.25 µm at the temperature range of 50-250 ℃, 5 ℃/$min$. Ionization energy was 70 eV.

### 1.4. Photocatalytic degradation

In the photocatalytic degradation of organic compounds, a wooden chamber was used which had a UVC lamp (15 w, Hitachi Co., Japan, wavelength of 256 nm) attached to the sidewall of the chamber (Fig. 2). 50 mL effluent with a optimal value of 0.1 g CuO NPs was placed in an ultrasonic bath for 5 min to obtain a suspension. The pH of the mixture was adjusted at the optimal pH of 6. Then, it was stirred at 500 rpm for 20 min to reach a uniform suspension. The sample was then transferred to a quartz tube 2 cm away from the UV source and exposed to UVC for 45 min. During the removal process, a quartz tube was attached to an oxygen capsule. At the end of the process, centrifugation (1000 rpm for 30 min) was applied to separate the solid phase from the liquid.

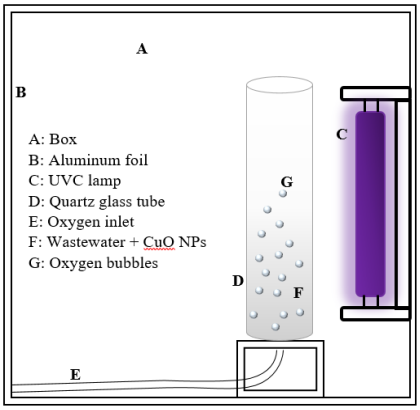


Fig. 2: Schematic representation of a photocatalytic reactor

### 2.5. Sonocatalytic process

In the sonocatalytic process, an ultrasonic bath (2200ETH, SONICA Co., Italy) with a capacity of 3 liters and a frequency of 40 kHz was employed (Fig. 3). 50 mL effluent was mixed with a optimal value of 0.1 g CuO NPs and stirred at 500 rpm for 20 min to reach a suspension. The pH of the mixture was adjusted at the optimal pH of 6. It was then transferred to an ultrasonic bath and treated with US waves ($40 \pm 5$ kHz for 45 min). In the next step, the nanoparticles were separated by a centrifuge.

As the aqueous phase can not be used in GC-MS, 20 mL effluent with 20 mL normal hexane (equal ratio) was transferred to an Erlenmeyer flask and stirred at room temperature for 24 h to achieve liquid-liquid extraction. The solution was then placed in a decanter funnel for 12 h to completely separate the aqueous phase from the organic one. Finally, effluent compounds were detected by GC-MS and the contaminant removal percentages were reported after studying chromatograms.

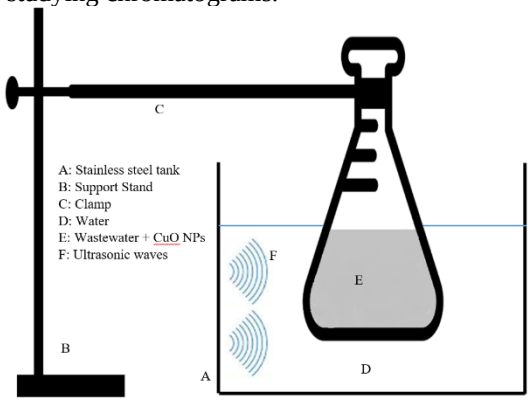


Fig. 3: Schematic representation of a sonocatalytic reactor

### 2.6. Removal mechanism

Upon exposure to UV or US waves, reductive electrons and oxidative holes will be generated in CuO nanoparticles, due to their narrow energy band as a result of the electrons excitation and transfer from the valence band (VB) to the conduction band (CB). The electron-hole pair reacts with the electron acceptor and electron-donor molecules to form Reactive Oxygen Species (ROS). These ROS will then react with organic molecules and break them down into simple compounds.

Sonochemistry refers to a chemical reaction in which a solution is exposed to US waves. It is indeed based on sonic cavitation, which involves the nucleation, growth, and collapse of microbubbles containing gas and steam, which eventually lead to light radiation. This phenomenon is called sonoluminescence (SL) (Pflieger et al., 2018). The emitted light leads to the pyrolysis of water molecules, giving rise to active radical species such as H° and OH° (Adewuyi, 2005) (Fig. 4). The main reactions of the removal of the organic compounds by UV and/or US wave in the presence the CuO NPs are given in Eqs. 1 to 10 and 11 to 15, respectively.

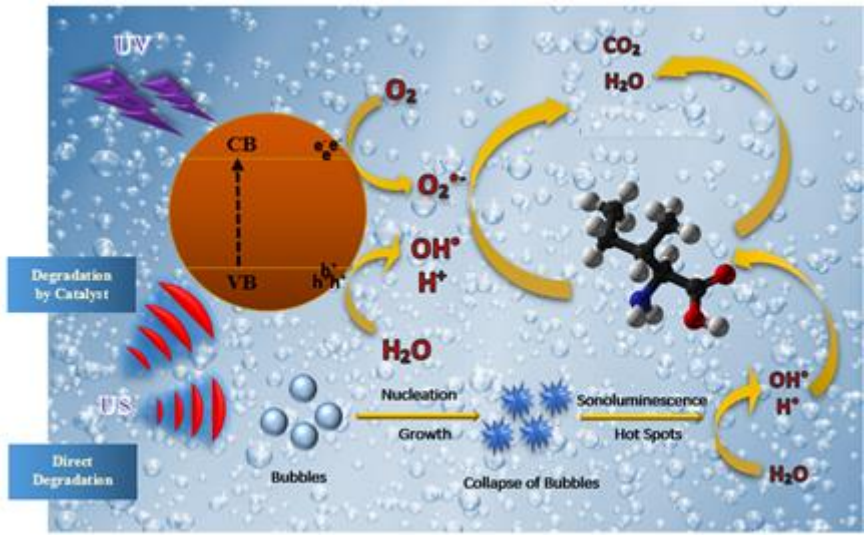


Fig. 4: Schematic overview of the mechanism of photocatalytic and sonocatalytic degradation

$$CuO\ NPs \xrightarrow{hv(UV\ or\ US)} e^- + h^+ \quad (1)$$

$$H_2O + h^+ \rightarrow OH^\circ + H^+ \quad (2)$$

$$O_2 + e^- \rightarrow O_2^{\circ-} \quad (3)$$

$$O_2^{\circ-} + H^+ \leftrightarrow HO_2^\circ \quad (4)$$

$$H_2O \leftrightarrow H^+ + OH^- \quad (5)$$

$$OH^- + h^+ \rightarrow OH^\circ \quad (6)$$

$$HO_2^\circ + O_2^{\circ-} \rightarrow HO_2^- + O_2 \quad (7)$$

$$HO_2^- + H^+ \rightarrow H_2O_2 \quad (8)$$

$$H_2O_2 + e^- \rightarrow OH^\circ + OH^- \quad (9)$$

$$H_2O_2 + O_2^{\circ-} \rightarrow OH^\circ + OH^- + O_2 \quad (10)$$

$$H_2O \xrightarrow{)))} H^\circ + OH^\circ \quad (11)$$

$$2OH^\circ \rightarrow H_2O_2 \quad (12)$$

$$(13)$$

$$H^\circ + O_2 \rightarrow HO_2^\circ \quad (14)$$

$$2HO_2^\circ \rightarrow H_2O_2 + 1/2O_2$$

$$Organic\ Compound + (O_2^{\circ-} or\ OH^\circ or\ HO_2^\circ) \rightarrow degradation\ product \rightarrow CO_2 + H_2O \quad (15)$$

## 2. Results and discussions

### 2.1. Properties of CuO NPs

Figure 5 shows the XRD pattern of CuO NPs which is in line with the standard JCPDS card no. of 89-5899. The peaks observed at the positions of 32.67°, 35.57°, 38.76°, 49.04°, 53.75°, 58.27°, 61.73°, 66.34°, 68.11°, 72.52°, and 75.37° correspond to the crystallographic planes of CuO. The intensity and narrow width of the peaks indicate the crystalline nature of the NPs (Khalili et al., 2020; Rajaei et al., 2013). Based on the Debay-Scherer formula (Eq. 16), the mean size of the crystallites was calculated from the width and position of the main peak in the XRD pattern as 84 nm.

$$D = K\lambda/\beta cos\theta \quad (16)$$

In this formula, $D$ is the average crystallite size, $K$ shows the crystal shape factor and is approximately 0.9. λ denotes the wavelength of the X-ray source (1.54 Å); $\beta$ is the peak width at half maximum height (FWHM) and θ is the diffraction angle (Rajaei et al., 2020; Safarkar et al., 2020).

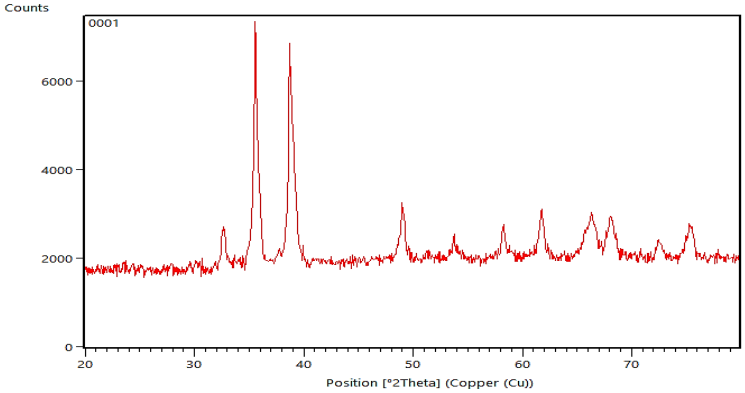


Fig. 5: XRD pattern of the synthesized CuO nanoparticles

Examination of the morphology of CuO nanoparticles by scanning electron microscopy revealed that the nanoparticles have a spherical structure (Manasa et al., 2021) (Fig. 6). Moreover, the average particle size was about 33 nm.

EDX spectroscopy was utilized to explore the purity of nanoparticles and their elemental composition. The intensity of the peaks is evidence of the formation of high-purity copper oxide nanoparticles (Fig. 7). Weak signals related to chlorine and carbon were in the spectrum are due to the use of copper chloride and biomaterials in the synthesis process (Velsankar et al., 2020). According to the results, Cu and O with the respective weight percentages of 22.62 and 77.38 and atomic percentages of 46.27 and 53.73 are the main elements constituting the sample.

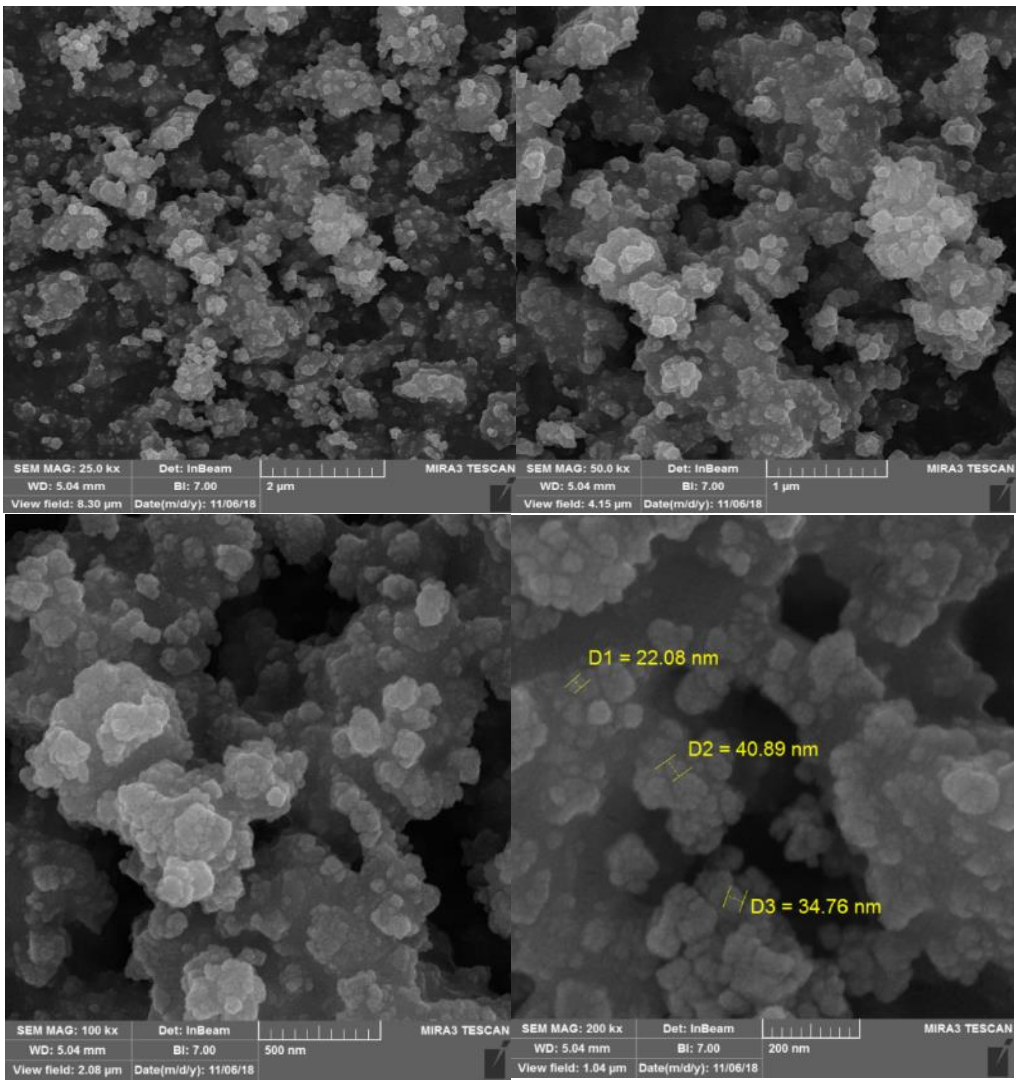

Fig. 6: SEM images of CuO nanocrystals with the scales of 1 µm, 2 µm, 200 nm, and 500 nm

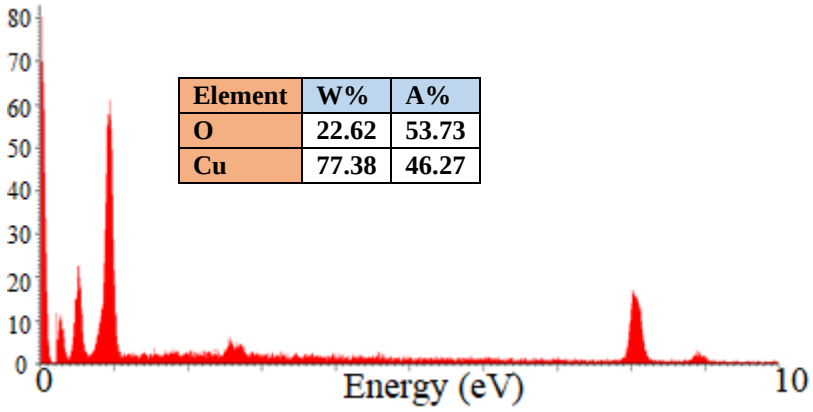


Fig. 7: Energy dispersive x-ray spectrum of CuO nanoparticles

### 2.2. Removal of organic compounds from the textile effluent

Organic compounds in the textile effluent sample of the treatment plant were identified by GC-MS (Table 1). The chromatogram of the effluent sample before the removal process is shown in Figure 8. The initial effluent sample contained Decane, Undecane, Dodecene, Naphthalene, decahydro-2,3-dimethyl, 2-methylmethylenecyclohexane, decahydro-1,5-dimethyl, Tridecane, Tetradecane, and Hexadecane which constituted 73% of the sample. They form the sample and are important components of the textile effluent (Table 2). Among the dissolved organic compounds, Dodecene with a frequency of about 19% exhibited the highest concentration of organic compounds.

Table 1: Organic compounds identified in the textile effluent by GC-MS

| Row | Compound | Retention time (min) | Frequency percentage |
|---|---|---|---|
| 1 | Benzene, ethyl- | 4.663 | 0.81 |
| 2 | XYLENE | 4.838 | 2.25 |
| 3 | Benzene, 1,2-dimethyl- | 5.396 | 0.64 |
| 4 | Nonane | 5.499 | 0.66 |
| 5 | Decane | 8.253 | 5.08 |
| 6 | 4-Pentyloxy-2,3-dicyanophenyl 4-Pentylcyclohexanecarboxylate | 10.747 | 0.47 |
| 7 | Undecane | 11.227 | 9.39 |
| 8 | Pentane, 2-isocyano-2,4,4-trimethyl- | 11.370 | 0.84 |
| 9 | 1,2,3,5-tetramethylcyclohexane | 12.205 | 0.74 |
| 10 | Naphthalene, decahydro-2,6-dimethyl- | 13.203 | 0.56 |
| 11 | Cyclopentane, (2-methylbutyl)- | 13.391 | 0.59 |
| 12 | 3-Propoxyamphetamine | 13.475 | 0.45 |
| 13 | trans,trans-1,10-Dimethylspiro[4.5]decane | 13.598 | 0.79 |
| 14 | Naphthalene, decahydro-1,6-dimethyl- | 13.650 | 0.58 |
| 15 | Naphthalene, decahydro-1,6-dimethyl- | 13.903 | 1.30 |
| 16 | Dodecane | 14.162 | 19.49 |
| 17 | Naphthalene, decahydro-1,6-dimethyl- | 14.344 | 2.99 |
| 18 | Naphthalene, decahydro-2,3-dimethyl- | 14.518 | 3.84 |
| 19 | Naphthalene, decahydro-2,6-dimethyl- | 14.609 | 1.69 |
| 20 | 2-methylmethylenecyclohexane | 14.927 | 5.39 |
| 21 | Naphthalene, decahydro-1,5-dimethyl- | 15.076 | 10.72 |
| 22 | Tridecane | 16.961 | 7.21 |
| 23 | Benzene, trimethyl(1-methylethyl)- | 17.447 | 0.65 |
| 24 | 4-tert-Butyl-1,2-dimethylbenzene | 17.700 | 0.57 |
| 25 | Tetradecane | 19.611 | 6.99 |
| 26 | Hexadecane | 24.484 | 5.38 |
| 27 | Decane, 2-methyl- | 28.883 | 0.84 |

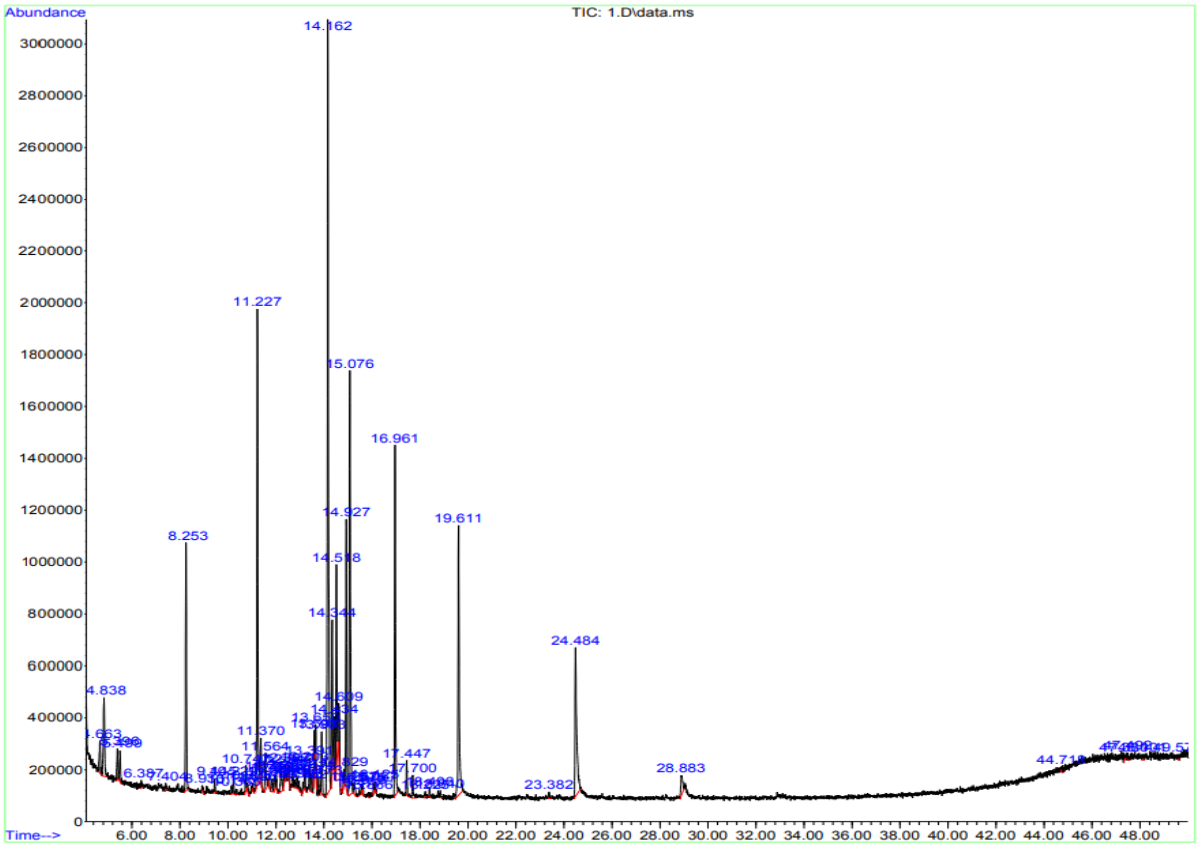


Fig. 8: Chromatogram of the textile effluent sample before the removal process

Table 2: Structural formula and frequency percentages of the main compounds identified in the effluent sample prior to the removal process

| Compound | Frequency percentage | Structural |
|---|---|---|
| Dodecene | 19.49 | |
| Naphthalene, decahydro-1,5-dimethyl- | 10.72 | |
| Undecane | 9.39 | |
| Tridecane | 7.21 | |
| Tetradecane | 6.99 | |
| 2-methylmethylenecyclohexane | 5.39 | |
| Hexadecane | 5.38 | |
| Decane | 5.08 | |
| Naphthalene, decahydro-2,3-dimethyl | 3.84 | |

First, the effect of photocatalytic process on the removal of organic compounds from the effluent was investigated. The chromatogram of the effluent sample exposed to UV waves in the presence of CuO nanoparticles is shown in Figure 9. Also, the frequency percentage of the identified organic compounds and their removal efficiency are listed in Table 3. According to the results, compounds such as 2-methylmethylenecyclohexane, naphthalene, decahydro-1,5-dimethyl, hexadecane, and decahydro-2,3-dimethyl were completely (100%) eliminated. Cyclic hydrocarbons are often degraded due to high pressure and instability in the face of hydroxyl radicals. Organic

compounds such as Tetradecane, Decane, Tridecane, Dodecene and Undecane were eliminated at the rate of 96.2, 94.0, 90.6, 88.3, and 87.7, respectively. In a study by Nouri Dodaran et al. in 2018, acceptable results were obtained in the removal of organic compounds from the effluent using the photocatalytic process (Nouri dodaran, 2018).

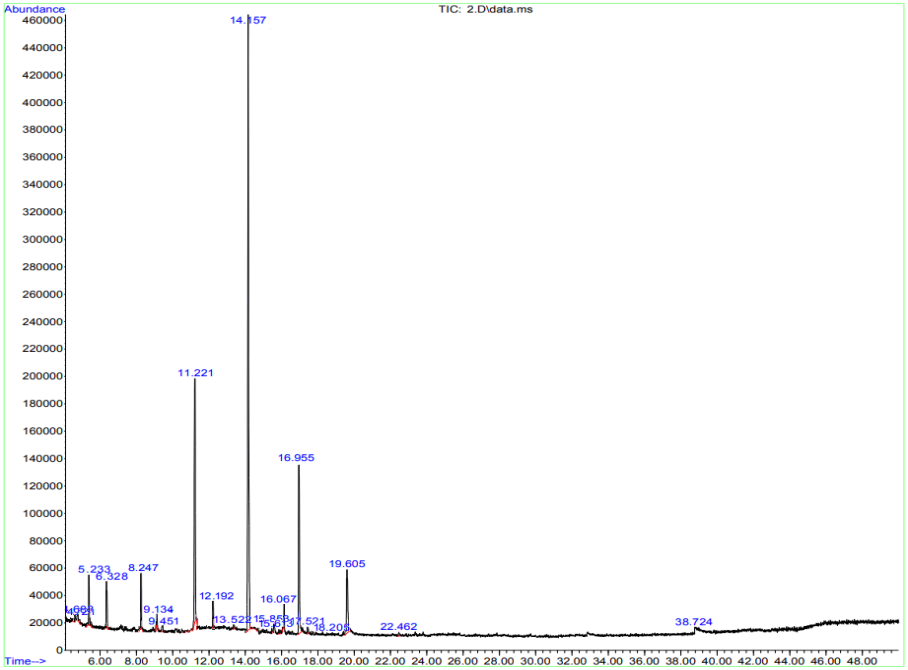


Fig. 9: Chromatogram of textile effluent sample after photocatalytic oxidation in the presence of CuO NPs and UV radiation

Table 3: Frequency and removal percentage of organic compounds in the textile effluent under the photocatalytic process

| Compound | Frequency percentage | Removal percentage |
|---|---|---|
| Undecane | 17.8 | 87.7 |
| Dodecene | 38.4 | 88.3 |
| Tridecane | 12.1 | 90.6 |
| Decane | 4.8 | 94.0 |
| Tetradecane | 5.3 | 96.2 |
| Naphthalene, decahydro-2,3-dimethyl | - | 100 |
| Hexadecane | - | 100 |
| 2-methylmethylenecyclohexane | - | 100 |
| Naphthalene, decahydro-1,5-dimethyl- | - | 100 |

According to the results of GC-MS and chromatogram of the textile effluent sample treated with US waves and CuO NPs (Fig. 10), the organic compounds in the effluent and their relative abundance are shown in Table 4. The results indicated that none of the target chemical compounds were fully eliminated. The highest removal efficiency was related to naphthalene, decahydro-2,3-dimethyl (approximately 84%) while the lowest removal rate was related to dodecene (52%). Figure 11 is reported for better comparison of the efficiency of photocatalytic and sonocatalytic processes in the removal of organic compounds from the textile effluent. According to the results, the UV waves in the presence of CuO nanoparticles were more efficient in the removal of different types of effluent organic compounds compared to the sonocatalytic process (CuO NPs/US).

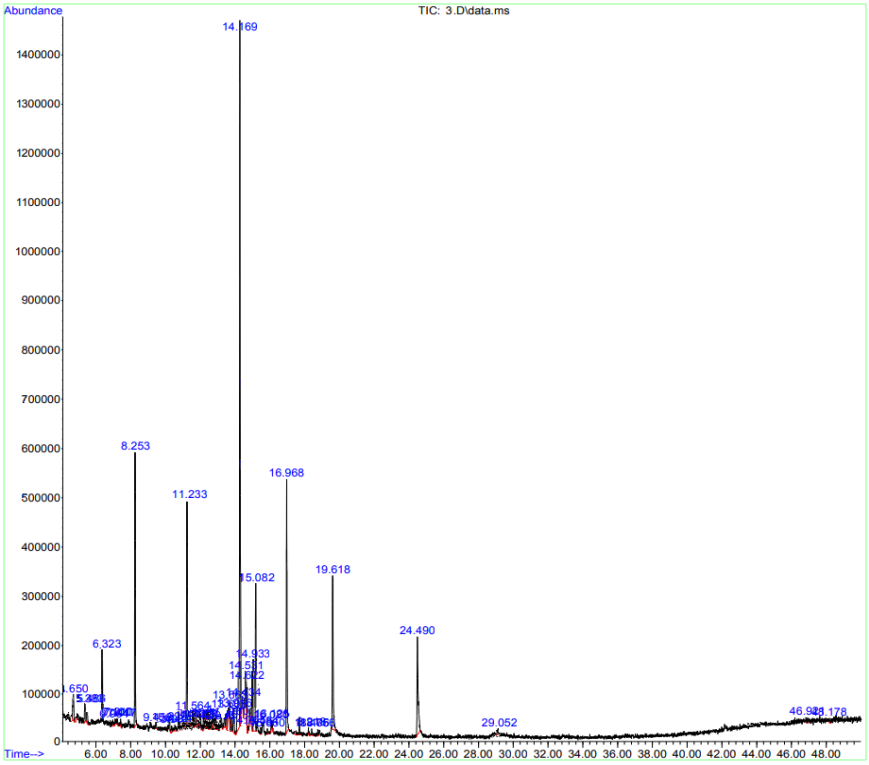


Fig. 10: Chromatogram of textile effluent sample after sonocatalytic process

Table 4: Frequency and removal percentage of organic compounds in the textile effluent by the sonocatalytic process

| Compound | Frequency percentage | Removal percentage |
|---|---|---|
| Dodecene | 25.1 | 52 |
| Tridecane | 8.8 | 61.3 |
| Decane | 10.1 | 63.6 |
| Hexadecane | 3.8 | 68 |
| Undecane | 7.4 | 70.9 |
| Tetradecane | 4.1 | 71.3 |
| Naphthalene, decahydro-1,5-dimethyl- | 4.5 | 79.2 |
| 2-methylmethylenecyclohexane | 2.6 | 81.6 |
| Naphthalene, decahydro-2,3-dimethyl | 2.3 | 83.5 |

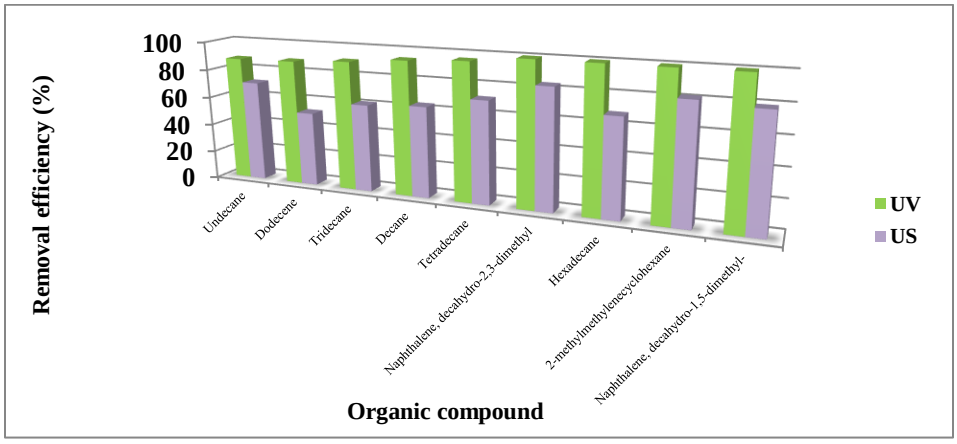


Fig. 11: Comparison of the efficiency of photocatalytic and sonocatalytic processes in the removal of organic compounds

## 3. Conclusion

In this study, copper oxide nanoparticles were first synthesized using *Peganum harmala* seed extract and then confirmed by XRD, EDX and SEM analyses. In the second stage, the efficiency of photocatalytic and sonocatalytic processes in the removal of organic compounds from the textile effluent of the treatment plant of Sabalan Textile Factory (Ardabil province) was tested. The results showed that the particles synthesized by green method are at the nanoscale with the mean size of 84 nm. The morphology of CuO nanoparticles was found spherical. Photocatalytic oxidation performance at an optimal contact time of 45 min and CuO NP dose of 0.1 g was 100% for the removal of 2-methylmethylenecyclohexane, naphthalene, and decahydro-2,3-dimethyl; while the highest organic compound removal efficiency in the sonocatalytic process under similar condition was 83.5%. According to the results, the photocatalytic process outperformed the sonocatalytic oxidation in the removal of all organic compounds as it exhibited higher degradation efficiency.

## Conflict of interest

The authors declare that they have no conflict of interest.

## References


Adewuyi, YG, (2005) Sonochemistry in environmental remediation. 2. Heterogeneous sonophotocatalytic oxidation processes for the treatment of pollutants in water. *Environmental science & technology*. 39(22): 8557-8570.

Ahmed, ESA, El-Sayed, BA, Mohamed, WA, Fahmy, A, Helal, A, (2021) Recycling of supported nanocomposites for hazardous industrial wastewater treatment via Solar photocatalytic process. *Egyptian Journal of Petroleum.* 30(2): 29-35.

Akerdi, AG, Bahrami, SH, (2019) Application of heterogeneous nano-semiconductors for photocatalytic advanced oxidation of organic compounds: a review. *Journal of Environmental Chemical Engineering*. 7(5): 103283.

Al-Zahrani, FA, El-Shishtawy, RM, Ahmed, NS, Awwad, NS, Hamdy, MS, Asiri, AM, (2020) Photocatalytic decolourization of a new water-insoluble organic dye based on phenothiazine by ZnO and TiO2 nanoparticles. *Arabian Journal of Chemistry.* 13(2): 3633-3638.

Arjaghi SK, Alasl MK, Sajjadi N, Fataei E and Rajaei GE, (2021) Green Synthesis of Iron Oxide Nanoparticles by RS Lichen Extract and its Application in Removing Heavy Metals of Lead and Cadmium. *Biological trace element research.* 199: 763-768.

Asgari G, Seidmohammadi A, Bagheri M, Chavoshi S, (2017) Evaluating the Efficiency of Dye Removal from Textile Industry Wastewater Using the Titanium Dioxide Photocatalytic Process under UV-LED Light Irradiation: A Case Study, Hamadan Nakh Rang Factory. *Scientific Journal of Hamadan University of Medical Sciences*. 24(2): 143-151.

Daneshvar, H, Dorraji, MS, Amani-Ghadim, AR, Rasoulifard, MH, (2019) Enhanced sonocatalytic performance of ZnTi nano-layered double hydroxide by substitution of Cu (II) cations. *Ultrasonics sonochemistry*. 58: 104632.

Ebrahimzadeh Rajaei G, Aghaie H, Zare K and Aghaie M, (2012) Adsorption of Ni (II) and Cd (II) ions from aqueous solutions by modified surface of Typha latifolia L. root, as an economical adsorbent. *Journal of Physical & Theoretical Chemistry*. 9: 137-147.

El Hakim, S, Chave, T, Nikitenko, SI, (2021) Sonocatalytic degradation of EDTA in the presence of Ti and Ti@ $TiO_2$ nanoparticles. *Ultrasonics Sonochemistry*. 70: 105336.

Fatimah, I, Nurillahi, R, Sahroni, I, Fadillah, G, Nugroho, BH, Kamari, A, Muraza, O, (2020) Sonocatalytic degradation of rhodamine B using tin oxide/montmorillonite. *Journal of Water Process Engineering*. 37: 101418.

Hasanpour, M, Hatami, M, (2020) Photocatalytic performance of aerogels for organic dyes removal from wastewaters: Review study. *Journal of Molecular Liquids*. 309: 113094.

Jamdagni, P, Khatri, P, Rana, JS, (2018) Green synthesis of zinc oxide nanoparticles using flower extract of Nyctanthes arbor-tristis and their antifungal activity. *Journal of King Saud University-Science*. 30(2): 168-175.

Khalili Arjaghi S, Ebrahimzadeh Rajaei G, Sajjadi N, Kashefi Alasl M and Fataei E, (2020) Removal of Mercury and Arsenic Metal Pollutants from Water Using Iron Oxide Nanoparticles Synthesized from Lichen Sinensis Ramalina Extract. *Journal of Health*. 11: 397-408.

Lam, SM, Sin, JC, Zeng, H, Lin, H, Li, H, Chai, YY, Choong, MK, Mohamed, AR, (2021) Green synthesis of Fe-ZnO nanoparticles with improved sunlight photocatalytic performance for polyethylene film deterioration and bacterial inactivation. *Materials Science in Semiconductor Processing*. 123: 105574.

Luque, PA, Nava, O, Soto-Robles, CA, Chinchillas-Chinchillas, MJ, Garrafa-Galvez, HE, Baez-Lopez, YA, Valdez-Núñez, KP, Vilchis-Nestor, AR, Castro-Beltrán, A, (2020) Improved photocatalytic efficiency of $SnO_2$ nanoparticles through green synthesis. *Optik*. 206: 164299.

Manasa, DJ, Chandrashekar, KR, Kumar, DM, Niranjana, M, Navada, KM, (2021) Mussaenda frondosa mediated facile green synthesis of Copper oxide nanoparticles-Characterization, Photocatalytic and their biological investigations. *Arabian Journal of Chemistry*. 14(6): 103184.

Nouri Dodaran, P, Fataei, E, Khanizadeh, B, (2019) Study on photocatalytic and sonocatalytic activity of Bi2O3 synthesized by Sol-gel method in removing organic

compounds of ardabil textile factory effluents. *Journal of Water and Wastewater*. 30(4): 67-77.

Pflieger, R, Gravier, L, Guillot, G, Ashokkumar, M, Nikitenko, SI, (2018) Inverse effects of the gas feed positioning on sonochemistry and sonoluminescence. *Ultrasonics sonochemistry*. 46: 10-17.

Rajaei GE, Aghaie H, Zare K and Aghaie M, (2013) Adsorption of Cu (II) and Zn (II) ions from aqueous solutions onto fine powder of Typha latifolia L. root: kinetics and isotherm studies. *Research on Chemical Intermediates*. 39: 3579-3594.

Rajaei GE, Khalili-Arjaghi S, Fataei E, Sajjadi N and Kashefi-Alasl M, (2020) Fabrication and characterization of polymer-based nanocomposite membrane modified by magnetite nanoparticles for $Cd^{2+}$ and $Pb^{2+}$ removal from aqueous solutions. *Comptes Rendus. Chimie*. 23: 563-574.

Rezaee-Mofrad MR, Miranzadeh MB, Pourgholi M, Akbari H, Dehghani R, (2013) Evaluating the efficiency of advanced oxidation methods on dye removal from textile wastewater. *Journal of Kashan University of Medical Sciences*. 17(1): 32-39.

Rezaei-Aghdam E, Shamel A, Khodadadi-Moghaddam M, Rajaei GE and Mohajeri S, (2021) Synthesis of $TiO_2$ and ZnO Nanoparticles and CTAB-Stabilized $Fe_3O_4$ nanocomposite: kinetics and thermodynamics of adsorption. *Research on Chemical Intermediates.* 47: 1759-74.

Safarkar R, Ebrahimzadeh Rajaei G and Khalili-Arjagi S, (2020) The study of antibacterial properties of iron oxide nanoparticles synthesized using the extract of lichen Ramalina sinensis. *Asian Journal of Nanosciences and Materials.* 3: 157-166.

Salavati, H, Tavakkoli, N, Hosseinpoor, M, (2012) Preparation and characterization of polyphosphotungstate/$ZrO_2$ nanocomposite and their sonocatalytic and photocatalytic activity under UV light illumination. *Ultrasonics Sonochemistry*. 19(3): 546-553.

Shahmoradi M, Gholami M, Mahaee M, Abouee Mehrizi E, Ghorbanpoor R, (2013) Investigation into organic matter and nutrient removal in an activated sludge wastewater treatment system: case study of Bojnurd. *Journal of North Khorasan University of Medical Sciences*. 5(5): 927-933.

Shashanka, R, Taslimi, P, Karaoglanli, AC, Uzun, O, Alp, E, Jayaprakash, GK, (2021) Photocatalytic degradation of Rhodamine B (RhB) dye in waste water and enzymatic inhibition study using cauliflower shaped ZnO nanoparticles synthesized by a novel One-pot green synthesis method. *Arabian Journal of Chemistry*. 14(6): 103180.

Velsankar, K, RM, AK, Preethi, R, Muthulakshmi, V, Sudhahar, S, (2020) Green synthesis of CuO nanoparticles via Allium sativum extract and its characterizations on antimicrobial, antioxidant, antilarvicidal activities. *Journal of Environmental Chemical Engineering*. 8: 104123.

Yusuff, AS, Popoola, LT, Aderibigbe, EI, (2020) Solar photocatalytic degradation of organic pollutants in textile industry wastewater by ZnO/pumice composite photocatalyst. *Journal of Environmental Chemical* Engineering. 8(4): 103907.